

Improved Dual Sinc Pulses to Reduce ICI Power and PAPR in OFDM-based Systems

Shaharyar Kamal¹, Hojin Kang², Cesar A. Azurdia Meza^{2*}, and Dong Seong Kim³

¹Department of Computer Science, Air University
Service Road E-9, Islamabad 44000, Pakistan
[e-mail: shaharyar.kamal@mail.au.edu.pk]

²Department of Electrical Engineering, Universidad de Chile
Santiago, 8370451, Chile

[e-mail: ho.kang.k@ing.uchile.cl, cazurdia@ing.uchile.cl]

³School of Electronic Engineering, Kumoh National Institute of Technology
Yanghოდong, Daehakro 61, 730-701, South Korea
[e-mail: dskim@kumoh.ac.kr]

*Corresponding author: Cesar A. Azurdia Meza

*Received February 10, 2020; revised October 28, 2020; revised November 20, 2020;
accepted November 26, 2020; published December 31, 2020*

Abstract

A new family of Nyquist-I pulses is proposed and named improved dual sinc pulse (IDSP). The IDSP is designed to improve performance in orthogonal frequency division multiplexing (OFDM)-based systems. The IDSP is a generalization of the dual sinc pulse (DSPP). This is because the DSP was formulated for $\alpha = 1$ whereas the IDSPP is valid for $0 \leq \alpha \leq 1$. The behavior of the IDSP is promising in terms of its frequency and time domain responses. Theoretical and numerical outcomes indicate that the IDSP outperformed other existing pulses applied in OFDM-based systems for various key evaluation metrics.

Keywords: Bit Error Rate, Frequency Offset, Nyquist-I Pulses, OFDM, Peak-to-Average Power Ratio(PAPR)

1. Introduction

Usage of data in cellular networks has increased significantly in the last few years, due to the growth of the smartphone industry. This is expected to increase even further with 5G and the hasty expansion of the Internet of Things (IoT). 5G application requirements such as lower latency, higher spectral efficiency, asynchronous transmission and higher peak data rate, cannot be achieved with the classical waveform in orthogonal frequency division multiplexing (OFDM), and so the design of the waveform for OFDM is an important problem that must be solved for 5G [1-5]. OFDM is characterized by high data transmission and bandwidth competence, multipath channel's stability, capability to convert a frequency selective fading channel into several nearly flat fading channels. Furthermore, OFDM mitigates the effect of delay spread using guard interval, and frequency domain equalization at the receiver side. These benefits make OFDM one of the fundamental technologies to apply in 5G cellular networks [6]. Also, most of the standards within wireless communication domain are based on OFDM systems, including digital video broadcasting (terrestrial), long term evolution, wireless fidelity, wireless personal area network, and worldwide interoperability for microwave access [7]. Recently, OFDM-based systems have been planned and implemented for information and power transfer within OFDM relay networks [5] and other wireless communication systems [8, 9]. Despite the benefits that OFDM-based schemes have, there are several shortcomings that need to be addressed properly to avoid performance degradation. Due to the focus of the work, OFDM-based systems are assumed unless stated otherwise.

1.1 Shortcomings of the OFDM-based systems

- Out-of-band (OOB) leakage: Communication among various users operating in the contiguous channels can be compromised due to high spectral side lobes interference. Such interference increases OOB [10, 11]. Diverse methods have been proposed to reduce the OOB power, such as symbol optimization [10], and frequency and time domain approaches [11]. However, these methods have high complexity, making their application infeasible in real life applications.
- Inter-carrier Interference (ICI): Performance is degraded by the effects of frequency mismatch between the receiver and transmitter oscillators, Doppler spread, and disturbance in the channel [12]. Moreover, such errors cause several problems including attenuation, rotation among the subcarriers, and ICI. Various methods are used to reduce ICI power such as frequency-domain equalization [13], time-domain windowing [14] and ICI self-cancellation [15]. Unfortunately, those methods are not sufficient to completely mitigate the problems in real applications.
- Peak-to-average Power Ratio (PAPR): OFDM-based technologies require numerous modulated subcarriers. When those subcarriers overlap in the frequency domain, a high rapid peak occurs in comparison to an average required peak, such high peak results in high PAPR [16]. This affects the performance of high power amplifiers (HPAs), analog to digital converters (ADC) and digital to analog converters (DAC). Furthermore, a non-linear distortion is introduced when the signal amplitude exceeds the limit of the HPA, which degrades the performance of the system with respect to PAPR and bit error rate (BER) [17]. Therefore, it is necessary to enable an OFDM system to work properly by minimizing PAPR and achieving low BER. Various methods have been proposed and implemented to reduce PAPR for OFDM-based systems such

as clipping and filtering, block coding, selective mapping and non-linear companding transform [16, 17], but these methods involve complexity at transmitter and receiver side in OFDM-based systems.

1.2 Problems Solution

In this manuscript, we proposed a pulse shaping technique to decrease OOB power, reduce ICI power, increase SIR power, minimize PAPR and provide low BER. From here on out this will be referred to simply as the objective conditions for the pulse. It involves simple processes without adding any complexity to an OFDM system. The pulse design includes three important aspects. First, a pulse should comply with Nyquist-I criterion to reduce channel interference [18]. Second, a pulse with a wider main lobe is necessary to diminish BER [19]. Third, pulses with smaller side lobes reduce ICI power [20], decreases OOB power [21] and minimizes PAPR [22].

1.3 Related Work

In the recent literature, various Nyquist-I pulses were proposed. One of those pulses is the improved modified Bartlett Hanning (IMBH) pulse. The IMBH was proposed to have low ICI power and BER [20]. Polynomial pulses showed sufficient reduction in OOB power [21]. Then, the improved parametric linear combination pulse (IPLCP) showed superiority in achieving lower PAPR and ICI power [22]. Recently, a new pulse, called dual sinc pulse (DSP) was proposed [23]. It is observed that the DSP is evaluated and investigated for a single value for the roll-off factor α , which is $\alpha = 1$. The DSP has a superior efficiency in terms of SIR and ICI power [23].

1.4 Contributions

- A distinct family of Nyquist-I pulses is proposed. This distinct family is termed improved dual sinc pulses (IDSPs), which is an improved version of the DSP [23], it introduces a new parameter i.e. a roll-off factor, α .
- An advantage of the proposed pulse is that the value for α is not set, while the DSP [23] was defined for only $\alpha = 1$. The IDSP analysis are made for various values of α , in particular for $\alpha = 0.22$ [22], which is found worth investigating in terms of the objective conditions for the pulse.
- To the author's best knowledge, it is the first time that the IDSP is examined in terms of OOB power, ICI power, SIR power, PAPR and BER, which will be referred to simply as the metrics from here on out. In the same way, readers are provided with a feasible solution to mitigate the drawbacks presented in OFDM-based schemes. This is done by designing and implementing a special pulse shaping function i.e. IDSP over DSP [23].
- The behavior of the IDSP is analyzed in terms of frequency and time domain responses for various quantities of the design parameters of the IDSP.
- The IDSP is compared to various proposed pulses e.g. IMBH [20], polynomial pulses [21] and IPLCP [22], in terms of the metrics. The polynomial pulses refer to Poly4, Poly5, and a linear combination of the Poly4 and Poly5 pulses, denoted as LCP45 [21].
- Performance of the IDSP and other existing pulses is evaluated for $\alpha = 0.22, 0.35,$ and 0.5 , through numerical and theoretical evaluations.

The rest of the manuscript is structured as follows. In Section II, a generic OFDM system is described and the evaluation metrics used in the manuscript are defined. In Section III, the IDSP is defined and its frequency and time response are analyzed. The performance of the IDSP and other existing pulses is investigated by using numerical and theoretical simulations in Section IV. Finally, conclusions of the work are given in Section V.

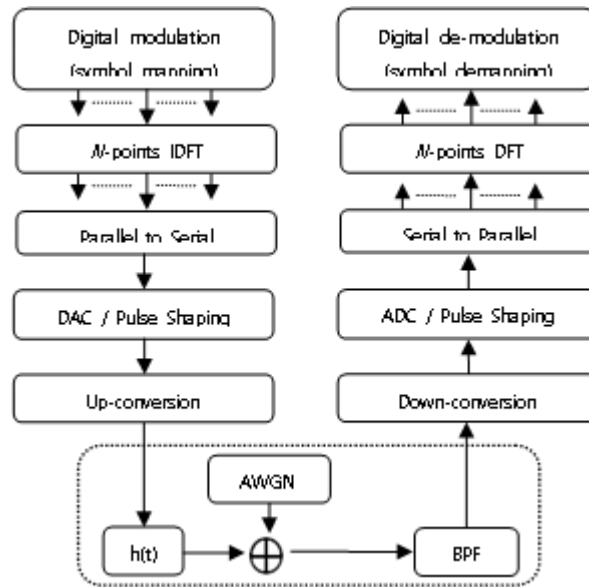


Fig. 1. N-subcarrier OFDM system

2. OFDM System Model

In this work we used a technique identified as pulse shaping and applied it to OFDM systems, as shown in Fig. 1. Modulation systems, such as M-PSK and M-QAM are used to modulate the data symbols. The inverse discrete Fourier transform (IDFT) processes the data symbols as inputs, and different frequencies are assigned to each subcarrier. After converting to serial data stream, the signal is transformed to time domain by using DAC. Here, the proposed IDSP is used at the transmitter side to produce a smooth analog signal to be transmitted through the channel. However, a reverse signal processing operation of the OFDM transmitter takes place at receiver. Furthermore, two key operations held at receiver side including a combination of radio frequency (RF) signal and band-pass filter (BPF) for processing, and elimination of frequencies above the Nyquist frequency through the use of ADC and the IDSP. Thus, the signal is converted to the frequency domain using the discrete Fourier transform (DFT) at the receiver side in OFDM system. A time limited pulse shaping expression, characterized by a time-domain N-subcarrier OFDM symbol, is expressed as:

$$x(t) = \sum_{k=-N/2}^{N/2-1} s_k p(t) e^{j2\pi f_k t} \quad (1)$$

where j is an imaginary unit, f_k is the frequency of the k th subcarrier, $p(t)$ is the pulse shaping expression, and s_k is the data symbol transmitted over the channel and characterized by zero mean and normalized average symbol energy. The conjecture that all data symbols are correlated is made [23], which complies with the following equation:

$$E[s_k s_m^*] = \begin{cases} 1, & \rightarrow k = m \\ 0, & \rightarrow k \neq m \end{cases} \quad (2)$$

where * is the complex conjugate. According to [18], $p(t)$ should be such that the subcarriers are orthogonal for OFDM systems defined as following:

$$\int p(t) e^{-j2\pi(f_k - f_m)t} dt = 0 \rightarrow k \neq m \quad (3)$$

To guarantee orthogonality amongst subcarriers, the subsequent equation must be fulfilled, which was shown as:

$$f_k - f_m = \frac{k - m}{T}, k, m = 0, 1, \dots, N - 1 \quad (4)$$

For N subcarriers, the orthogonality is satisfied by $(1/T)$, which is the least subcarrier frequency spacing.

2.1 OOB Power

Large side lobes in the frequency domain introduce undesirable interference among the adjacent channels operated by multiple users, which eventually increase OOB power. OOB power can be decreased through pulse shaping. In the frequency domain, $x(t)$ from (1), becomes as given in [21]:

$$X(f) = \sum_{k=-N/2}^{N/2-1} s_k P\left(f - \frac{k}{T}\right) \quad (5)$$

where $P(f)$ is the Fourier transform of the pulse shaping function $p(t)$ that is given in (1). The average power spectral density (PSD) of the $X(f)$ is denoted as $P_{PSD}(f)$ and is given by:

$$P_{PSD}(f) = E\{|X(f)|^2\} \quad (6)$$

and the average PSD of an OFDM signal becomes [21]:

$$P_{PSD}(f) = \sum_{k=-N/2}^{N/2-1} \left| P\left(f - \frac{k}{T}\right) \right|^2 \quad (7)$$

where the $P_{PSD}(f)$ is used to evaluate the OOB power of the different pulses.

2.2 ICI, SIR, BER, and PAPR Evaluation Metrics

Carrier frequency offset results in ICI and degrades the performance of OFDM systems. Therefore, the efficiency of OFDM systems is determined by considering a frequency offset,

Δf , with respect to ICI power, SIR power, and BER. An additive white Gaussian noise (AWGN) process with zero mean and variance of $N_0/2$ per dimension, which is a complex noise, is considered in the channel.

An ideal channel, i.e. $h(t) = \delta(t)$, is considered to analyze the outcome of frequency offset on ICI. Furthermore, the BPSK-OFDM system is used to compare and evaluate performance of existing pulses, including IDSP, over an AWGN channel in terms of ICI power, SIR power and BER [19]. These metrics depend on the frequency offset, Δf . The average ICI power across different sequences is defined as [19]:

$$\overline{\sigma_{ICI}^m} = \sum_{\substack{k=0, \\ k \neq m}}^{N-1} \left| P\left(\frac{k-m}{T} + \Delta f\right) \right|^2 \quad (8)$$

The signal-to-interference power ratio (SIR) is defined in [19] as follows:

$$SIR = \frac{|P(\Delta f)|^2}{\overline{\sigma_{ICI}^m}} \quad (9)$$

The BER is analyzed by using BPSK-OFDM over a channel that considers AWGN and frequency offset to evaluate various pulse shaping functions in terms of BER [19, 21-24]. The BER expressions are the following:

$$\overline{BER}_{OFDM} = 1 - (1 - BER_{symbol})^N \quad (10)$$

$$BER_{symbol} = \frac{1}{2} \left(\frac{Q(\cos\theta [P(-\Delta f) + \sqrt{P_{ICI}}] \sqrt{2\gamma_b}) + Q(\cos\theta [P(-\Delta f) - \sqrt{P_{ICI}}] \sqrt{2\gamma_b})}{Q(\cos\theta [P(-\Delta f) + \sqrt{P_{ICI}}] \sqrt{2\gamma_b})} \right) \quad (11)$$

Further details and derivation of the BER expressions in (10) and (11) are given in [25]. It can be seen from (10) and (11) that the average BER is specified as a function of average ICI power, P_{ICI} , frequency offset, Δf , phase noise, θ , number of subcarriers N , and $\gamma_b = E_b/N_0$.

PAPR for the pulse shapes is measured in the frequency domain, as it was done in [22]. The total PAPR is given by the modulation arrangement and the pulse shaping function [22].

3. Improved Dual Sinc Pulses

In this Section, a newfangled pulse shaping function is proposed and called improved dual sinc pulse (IDSP). The newfangled pulse is designed to fulfil the objective conditions. This pulse is an improved version of DSP [23]. The IDSP considers a roll-off factor, α , with range $0 \leq \alpha \leq 1$. In this work, IDSP is evaluated for various values of α including $\alpha = \{0.35, 0.5\}$, in particular for $\alpha = 0.22$ [22]. Because those values are considered important through performance point of view in the recent literature [18-23]. The IDSP representation in the frequency domain, $P_{IDSP}(f)$, is defined as follows:

$$P_{IDSP}(f) = \{\beta \sin c(fT) \times [(1 - \beta) \sin c(\alpha\gamma fT)]^2\}^n \quad (12)$$

The design parameters in the IDSP i.e. β , γ , and n are defined as real numbers. β controls the width of the main lobe's upper part, γ controls the phase of a pulse and helps in diminishing the side lobes, and n is the power of IDSP. These extra degrees of freedom are used to meet the objective conditions for the pulse. The Nyquist-I criterion is given in the frequency-domain through the following expression:

$$P(f) = \begin{cases} 1, & \rightarrow f = 0 \\ 0, & \rightarrow f = \pm 1/T, \pm 2/T, \dots \end{cases} \quad (13)$$

For $f = 0$, the IDSP is examined with generic values of α , β , γ , and n , to confirm that the IDSP fulfills the frequency domain condition of the Nyquist-I criterion, given in (13). For this specific case, the result is always equal to one. Moreover, when the IDSP is examined for $f = \pm 1/T, \pm 2/T, \dots$, and again considering general values for α , β , γ and n , the IDSP is equal to zero. Thus, the proposed pulse defined in (12) satisfies the condition of the Nyquist-I criterion. The performance of the pulses is analyzed in the time and frequency domain. The purpose of designing the IDSP includes:

- To eradicate the limitations of DSP [23], which was defined for only, $\alpha = 1$.
- Determine the performance of IDSP for small values of α , in particular $\alpha = 0.22$. This is because $\alpha = 0.22$, was suggested by the 3rd Generation Partnership Project (3GPP) for pulse shaping filters [22].
- The optimum values of β , γ , and n depend on the roll-off factor, α , and the modulation scheme.
- To fully validate the achievement of the IDSP pulse, we compare its performance with other state-of-the art pulses for $\alpha = \{0.22, 0.35, 0.5\}$ and for various performance metrics.
- The frequency response for IDSP is simple in comparison with other current pulses [20-22]. Furthermore, such simple frequency response expression is desirable to reduce complexity in OFDM-based system.

The proposed IDSP filter is evaluated in the frequency domain by varying β and γ for a fixed n and α in Fig. 2 and Fig. 3. The main lobe of the IDSP becomes wider with an increase in β . Moreover, a change is noticed in the upper part of the main lobe by tuning β values, as shown in Fig. 2. Therefore, such significance of β is important because a narrow main lobe degrades the performance of the system in terms of higher BER values [19].

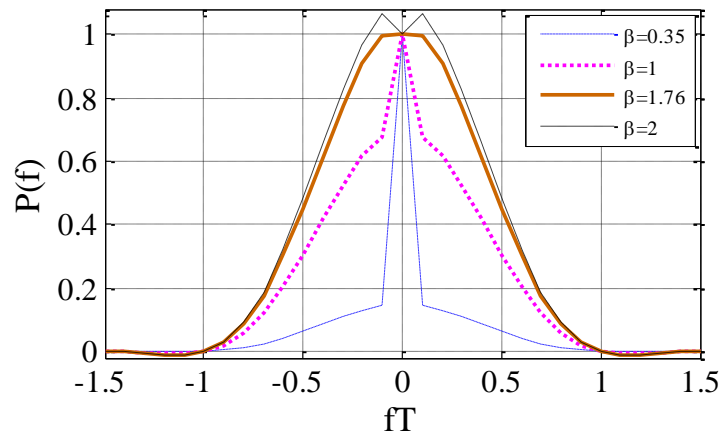


Fig. 2. Frequency response of the IDSP filter as β differs for $\gamma = 3, n = 1$ at $\alpha = 0.22$

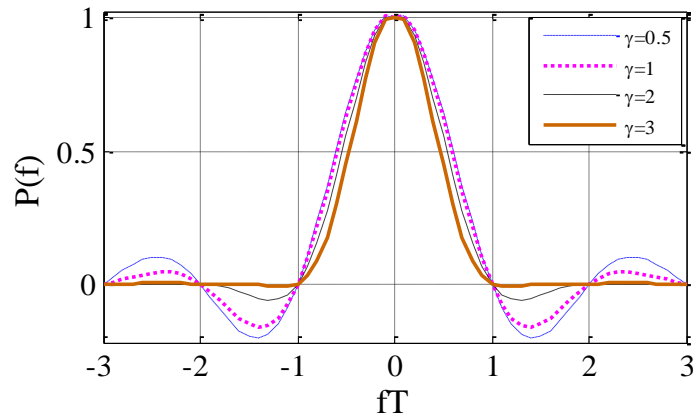


Fig. 3. Frequency response of the IDSP filter as γ differs for $\beta = 1.76, n = 1$ at $\alpha = 0.22$

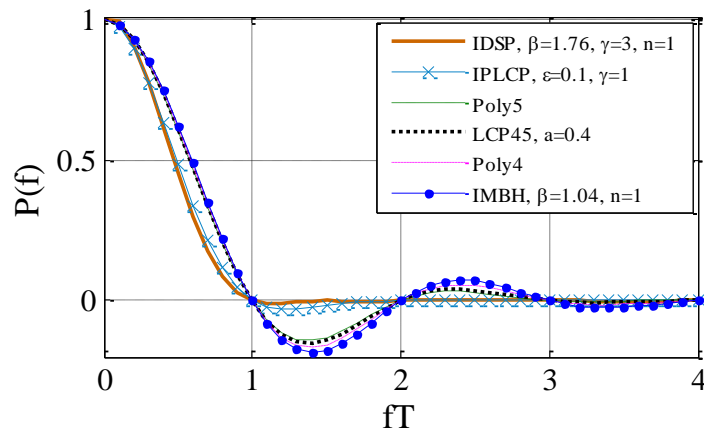


Fig. 4. Frequency function of the IDSP and other assessed pulse shaping functions for $\alpha = 0.22$

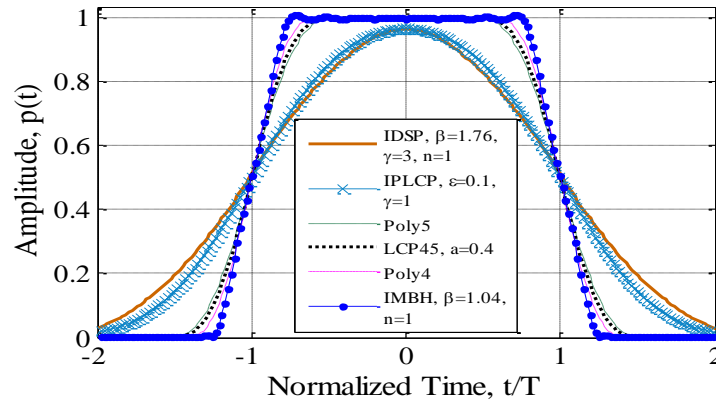


Fig. 5. Time function of the IDSP and other assessed pulse shaping functions for $\alpha = 0.22$

Fig. 3 shows that the side lobe's magnitude for the IDSP decreases as the value of γ increases. Moreover, a reduction in the side lobes of a pulse is desirable in reducing ICI power and PAPR [21, 22]. **Fig. 4** depicts a comparison of frequency function of the IDSP and other comparison pulses. The comparison pulses showed best performance at the particular values of their design parameters, is the reason why we selected those values. The proposed pulse shows the smallest side lobes whereas IMBH has the largest magnitude side lobes. We assume that the proposed pulse can greatly reduce OOB power, ICI power and PAPR due to a sufficient decrease in the lateral side lobes of IDSP frequency response, which will be further discussed in the next section. **Fig. 5** shows that the IDSP has a triangular shape in time domain. This is because of the reduced magnitude in the side lobes of the filter's frequency response, as shown in **Fig. 4**. Moreover, there is a trade-off between time and frequency domain pulse shaping, which can be understood by observing the behavior of the IMBH pulse, which shows high magnitude side lobe in frequency domain and has a rectangular form in time domain, as depicted in **Fig. 4** and **Fig. 5**.

We examined the frequency-domain close form expression of the IDSP by changing the value of one parameter whilst maintaining the others constant. When the β value changes and other parameters values are fixed i.e. $\gamma = 3$ and $n = 1$, the central lobe widens at high value of β . For the case of $\beta = 1.76$ and $n = 1$, and the value of γ differs, it is shown that a high value of γ produces a significant reduction in the side lobe's magnitude. Therefore, $\beta = 1.76$, $\gamma = 3$, and $n = 1$ for IDSP at $\alpha = 0.22$, is considered satisfactory according to the theory proposed and implemented for wider main lobe in [19, 20] and smallest magnitude side lobes in [22, 23], as shown in **Fig. 2** and **Fig. 3**, respectively. We investigated $\beta = 1.76$, $\gamma = 3$ and $n = 1$ for the IDSP at $\alpha = \{0.22, 0.35, 0.5\}$, in terms of several evaluation metrics. Although, the ideal quantity of β and γ may vary for various α values.

4. Simulation Results and Discussion

We compare IDSP with other existing pulses i.e. IMBH, IPLCP, Poly4, Poly5 and LCP45 in terms of several evaluation metrics. These pulses have explicit frequency domain expressions and showed best performance at particular values of their design parameters [20-22]. We examine the IDSP and other state-of-the-art pulses in terms of OOB power and BER through theoretical simulations. We employed the pulses in a real scenario, evaluating them with respect to the performance metrics (ICI power, SIR power and PAPR) using numerical simulations and according to the parameters given in **Table 1**.

A sub-optimum value for β is investigated with numerical and theoretical simulations with respect to ICI power and BER for $\alpha = 0.22$. This value for β is based on two important factors for OFDM-based systems. First, the value should have small side lobes to decrease OOB power, reduce ICI power, increase SIR power, and minimize PAPR. Second, the value should keep a wider main lobe in order to achieve low BER value. Here, the sub-optimum β means that β value is evaluated by using numerical and theoretical simulations. However, analytically obtaining the optimal value for β seems currently unrealizable.

The increase in OOB power is related to large side lobes in the frequency domain, which eventually results in unwanted interference in OFDM-based systems. Side lobes with small magnitude reduce the OOB power [21]. Therefore, the achievements of the IDSP and other existing pulses are evaluated in terms of OOB power using (7) via theoretical simulation, shown in Fig. 6. We observe that the IDSP shows the lowest OOB power whereas IMBH has high OOB power. The difference between the IDSP and the IMBH is 7dB.

Next, the achievements of the IDSP and other well-known pulses, in terms of ICI power are evaluated through numerical simulations. In-addition, we used an AWGN channel in a 64 subcarrier OFDM-based system. We used binary phase shift keying (BPSK) in the OFDM system to validate the results with respect to ICI power and SIR power [20, 22, 23].

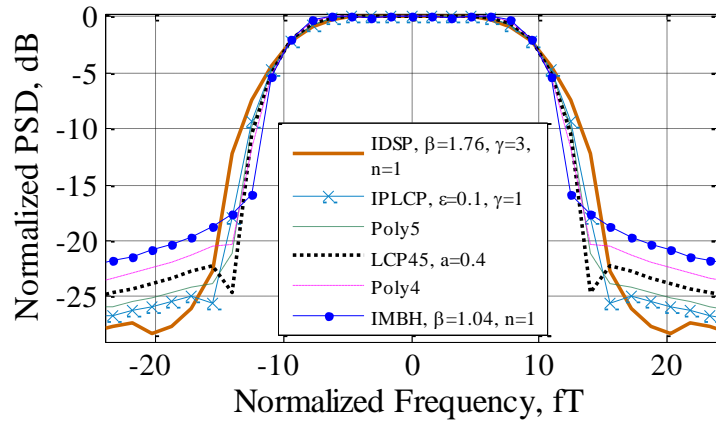


Fig. 6. Theoretical OOB power of IDSP, and other pulses assessed in a 64 subcarriers OFDM system, at $\alpha = 0.22$

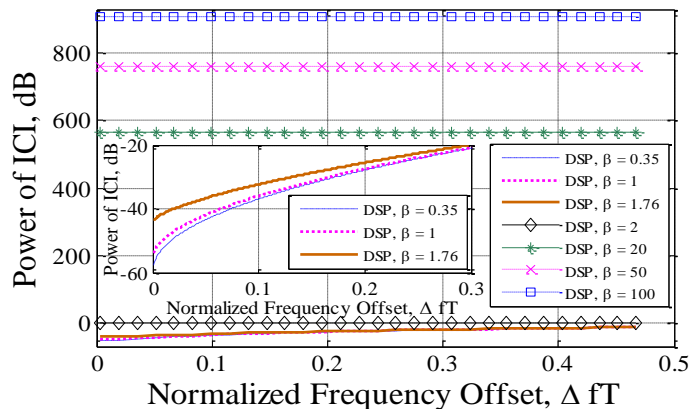


Fig. 7. ICI power of IDSP assessed in a 64 subcarrier OFDM system for $\gamma = 3, n = 1$, as β differs at $\alpha = 0.22$

We consider the study of the ICI power in two ways i.e. finding a sub-optimum value of β for the IDSP and comparing its performance to other pulses in terms of ICI power at $\alpha = 0.22$. The value of β is investigated by running extensive computer simulations, shown in Fig. 7, where various β values are considered as an example. It is observed that $\beta = 0.35$ shows lowest ICI power, while $\beta = 100$ has maximum ICI power for OFDM-based system. The values i.e. $\beta \geq 2$ should be ignored because it shows maximum ICI power. Furthermore, the amplitude of the IDSP seems disturbing at $\beta = 2$ whereas $\beta = 0.35$ and 1 show narrow main lobe in Fig. 2. The only value of $\beta = 1.76$ shows sufficient performance in reducing ICI power by having narrow side lobes and a wide main lobe for IDSP, obvious in Fig. 4. The IDSP at $\beta = 1.76$, $\gamma = 3$, $n = 1$ shows better achievements with respect to ICI power.

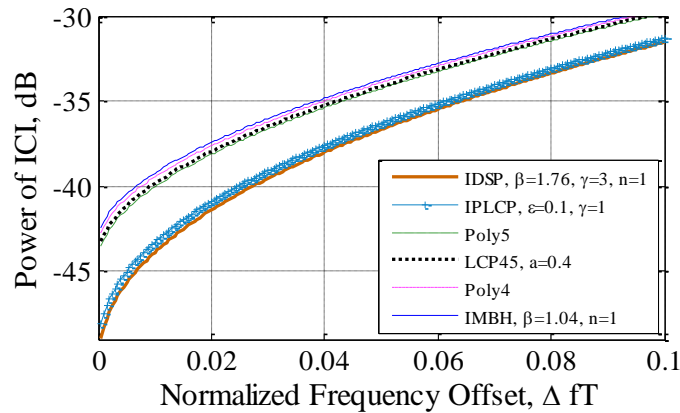


Fig. 8. ICI power of various pulses assessed in a 64 subcarrier OFDM system for $\alpha = 0.22$

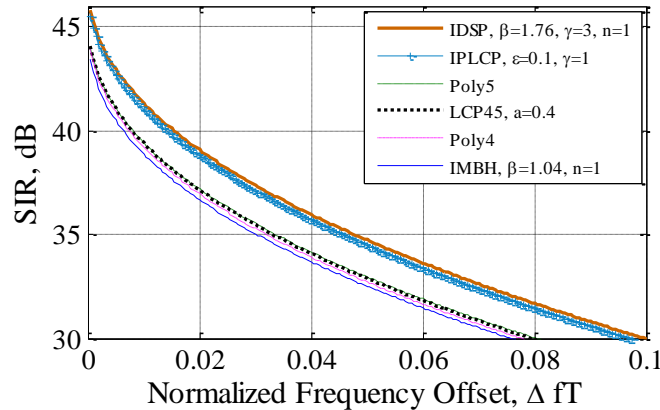


Fig. 9. SIR power of various pulses using a 64 subcarrier OFDM system for $\alpha = 0.22$

However, it is also necessary to verify that widening the main lobe lowers BER [19] to approve the value for β in terms of BER. Therefore, the $\beta = 1.76$, $\gamma = 3$, $n = 1$, are also required to be assessed in terms of BER for a given roll-off factor and transmission scheme.

Fig. 8 depicts a comparison of the IDSP and other current pulses that are employed in OFDM-based system with a normalized frequency offset, ΔfT , in terms of ICI power at $\alpha = 0.22$. It shows that the proposed pulse has minimum ICI power, whereas IMBH achieves maximum ICI power among the other pulses, for all normalized frequency offsets, ΔfT , considered. In-addition, it verifies that pulses with small side lobes shows sufficient decrease

in the ICI power [19-23].

Table 1. Simulation Parameters for ICI, SIR, and PAPR Power

Parameter	Value
Modulation	BPSK, 16QAM
Number of Symbols	100
Number of Subcarriers	64
Input Data Block Size	64
Transmission Bandwidth	20MHz
Block Oversampling	4
Bit-to-noise ratio	30dB
Roll-off factor, α	0.22, 0.35, 0.5

The IDSP shows maximum SIR power among the assessed pulses, as shown in Fig. 9. Different pulses are employed in a 64-subcarrier OFDM system in terms of SIR power at $\alpha = 0.22$. The numerical results are obtained during simulations for small and large ΔfT . The SIR power of the proposed pulse is 27.81 dB for $\Delta fT = 0.15$, which is higher than the SIR power of IPLCP, Poly5, LCP45, Poly4 and IMBH pulses i.e. 27.56, 26.24, 26.11, 26.03, 25.93 dB, respectively. Moreover, the SIR power of IDSP for $\Delta fT = 0.35$, is 16.30 dB, which is also higher than the SIR power of IPLCP, Poly5, LCP45, Poly4 and IMBH pulses i.e. 16.21, 15.66, 15.60, 15.54, 15.48 dB, respectively. Hence, the numerical results indicate that the IDSP has superior results in terms of SIR power for OFDM-based system.

BER comparative analysis of the IDSP and other existing pulses are based on BPSK-OFDM system over an AWGN channel, using expressions given in (10) and (11) and via theoretical simulations. Further details regarding the BER expressions can be found in [19, 21-25]. The BER comparative analysis is based on two findings i.e., to determine the sub-optimum value of β , and evaluate the performance of the IDSP and other assessed pulses for $\alpha = 0.22$. Fig. 10 depicts a comparison of different values of β for the IDSP at $\Delta fT = 0.15$, $\theta = 10^\circ$ and $\alpha = 0.22$. Where, only particular values of β i.e. $\beta = 0.35$, 1 and 1.76, are considered. Because $\beta = 0.35$, 1 and 1.76 reduced ICI power more significantly, which can be seen in Fig. 7. The $\beta = 0.35$ and 1 show highly reduced ICI power, but both β values are not able to minimize BER sufficiently, whereas $\beta = 1.76$ achieves low BER, as seen in Fig. 10. This shows that there is a relation between narrower main lobes and higher BER [19]. In particular a main lobe with narrow upper part, which is obvious from Fig. 2. To $\beta = 0.35$ and 1 had narrow main lobes and high BER, as shown in Fig. 10. Therefore, the IDSP with $\beta = 1.76$, $\gamma = 3$, and $n = 1$, performs well with respect to ICI power and BER, with $\alpha = 0.22$. Moreover, $\beta = 1.76$, $\gamma = 3$, $n = 1$, are used throughout the rest manuscript, which shows that it is a suitable combination for roll-off factor $\alpha = 0.22$ and the OFDM transmission system.

The performance of the pulses is compared in terms of BER over an AWGN channel, using a OFDM system with 64 subcarriers, for normalized frequency offset, $\Delta fT = \{0.15, 0.3\}$, $\theta = 30^\circ$ and $\alpha = 0.22$, as shown in Fig. 11 and Fig. 12. IMBH shows wider main lobe with large magnitude side lobes in Fig. 4, and it has achieved the lowest BER whereas IPLCP shows high BER among all the pulses, as depicted in Fig. 11 and Fig. 12. The IDSP only performs better than IPLCP, in terms of BER at small normalized frequency offset value i.e. $\Delta fT = 0.15$. When the normalized frequency offset is increased i.e. $\Delta fT = 0.3$, the IDSP showed better performance by achieving low BER than IPLCP and Poly5. It shows that the proposed pulse performs better when frequency offset increases, shown in Fig. 12. IMBH achieves better results than existing pulses in terms of BER for the normalized frequency offsets considered,

due to wider main lobe and larger side lobes, as obvious in Fig. 4.

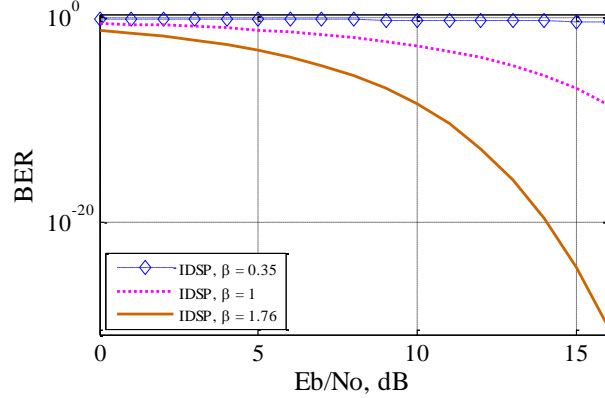


Fig. 10. Theoretical BER of IDSP for a 64 subcarriers OFDM system for $\gamma = 3$, $n = 1$, and varying β value for $\Delta fT = 0.15$, $\theta = 10^\circ$, and $\alpha = 0.22$

However, there is a tradeoff between ICI power and BER [19-23]. The IDSP is designed in such a way that it provides a balance between the metrics for OFDM-based systems. The ICI power minimizes when the output side lobes of a frequency response is reduced [19-23]. Reducing the side lobes affects the main lobe of a pulse because smaller side lobes allow narrower main lobes, shown in Fig. 4. Having a narrower main lobe increases BER while such state highly reduces the ICI power of a system [23]. After studying IDSP with respect to ICI power and BER, it is observed that the IDSP is a unique pulse that provides an effective tradeoff between this metrics.

The performance of the pulses is assessed in terms of PAPR, as it was done in [22]. The PAPR is measured in the frequency domain of various pulse shaping functions. Furthermore, the total PAPR value considers the modulation scheme and pulse shaping function, and 10^5 OFDM system blocks were simulated [22]. Smaller side lobes result in lower PAPR [22]. In Fig. 4, it is obvious that the proposed IDSP has the smallest side lobes. It is also shown that the proposed pulse can lower PAPR.

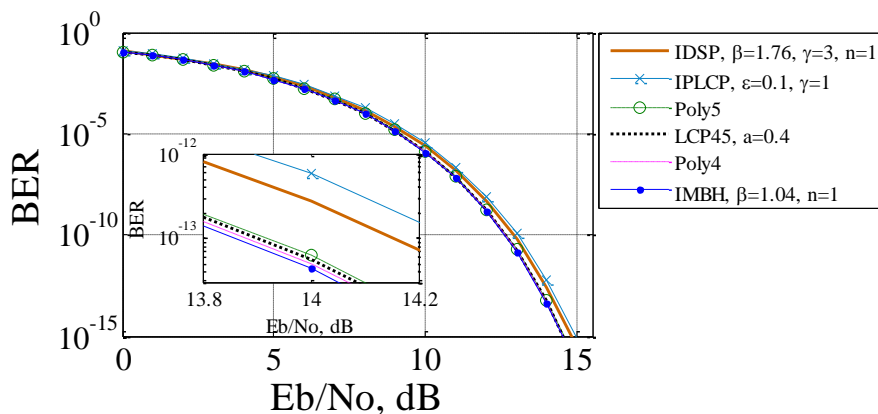


Fig. 11. Theoretical BER of IDSP and other pulses for a 64 subcarriers OFDM system for $\Delta fT = 0.15$, $\theta = 30^\circ$, and $\alpha = 0.22$

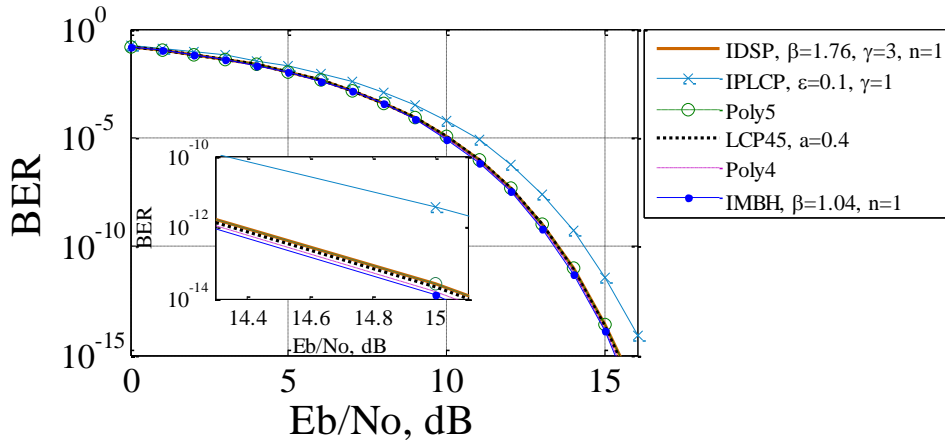


Fig. 12. Theoretical BER of IDSP and other pulses for a 64 subcarrier OFDM system for $\Delta fT = 0.3$, $\theta = 30^\circ$, and $\alpha = 0.22$

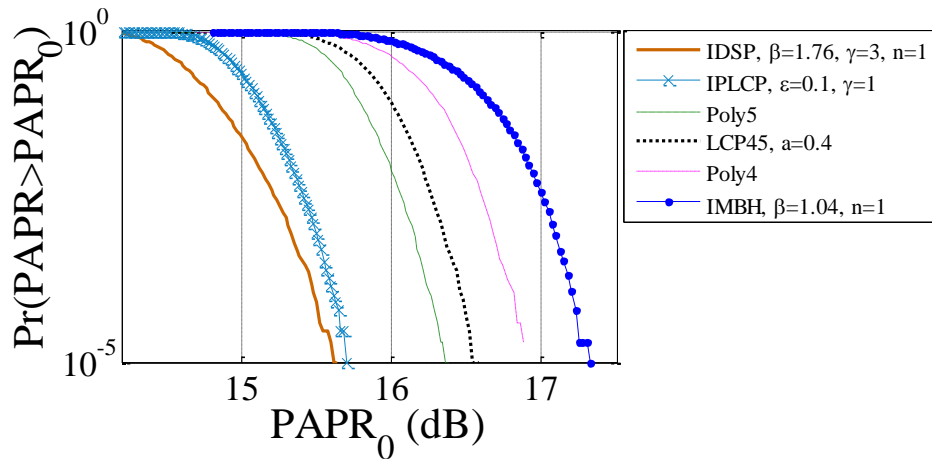


Fig. 13. CCDF of PAPR for different assessed pulses using 16-QAM and an OFDM system for $\alpha = 0.22$

Therefore, the performance of pulses is compared by employing their time domain response expression at the transmitter side using 16-QAM, in terms of PAPR using numerical simulations, as shown in **Fig. 13**. Results are given as empirical complementary cumulative distribution function (CCDF) of the PAPR versus the threshold PAPR ($PAPR_0$). The parameters used in the simulations to measure PAPR are presented in **Table 1**. The IDSP achieves the highest PAPR reduction for the pulses considered, as shown in **Fig. 13**. Moreover, IMBH shows the highest PAPR value, which verifies that pulses with larger side lobes result in high PAPR [22]. The IDSP is superior to existing pulses in terms of the metrics for OFDM system at $\beta = 1.76$, $\gamma = 3$, $n = 1$ and $\alpha = 0.22$.

Performance for the pulses is also discussed for different roll-off factors, $\alpha = \{0.35, 0.5\}$, in terms the metrics via theoretical and numerical simulations, as it was done for $\alpha = 0.22$. It is noticed that for $\beta = 1.76$, $\gamma = 2$, $n = 1$ for $\alpha = \{0.35\}$, and $\beta = 1.76$, $\gamma = 1.6$, $n = 1$ for $\alpha = \{0.5\}$, the IDSP outperforms other pulses in terms of the metrics.

Table 2. Average Power Spectral Density at Normalized Frequency = ± 18 , Average ICI & SIR Power at Normalized Frequency Offset = 0.2, and Average PAPR at $PR(PAPR > PAPR_0) = 10^{-3}$, for different pulses and $\alpha = \{0.35, 0.5\}$

Pulse	OOB power, dB	ICI power, dB	SIR power, dB	PAPR, dB	α
IDSP	-35	-25.01	23.60	15.21	0.35
IPLCP	-33	-24.63	23.17	15.25	
Poly5	-32	-24.01	22.30	15.62	
LCP45	-29	-23.96	22.28	15.73	
Poly4	-27	-23.92	22.15	15.88	
IMBH	-24	-23.80	21.85	16.24	
IDSP	-31	-25.88	23.62	15.19	0.5
IPLCP	-27	-25.57	23.31	15.21	
Poly5	-28	-24.95	22.52	15.24	
LCP45	-25	-24.92	22.44	15.26	
Poly4	-23	-24.84	22.41	15.29	
IMBH	-19	-24.63	22.09	15.50	

Table 3. Average BER for different pulses for SNR = 14dB

Pulse	BER	ΔfT	α
IDSP	4.78×10^{-2}	0.15	0.35
IPLCP	5.42×10^{-2}		
Poly5	4.63×10^{-2}		
LCP45	4.60×10^{-2}		
Poly4	4.56×10^{-2}		
IMBH	4.46×10^{-2}		
IDSP	7.32×10^{-2}	0.3	0.35
IPLCP	9.76×10^{-2}		
Poly5	7.33×10^{-2}		
LCP45	7.25×10^{-2}		
Poly4	7.12×10^{-2}		
IMBH	6.83×10^{-2}		
IDSP	5.04×10^{-2}	0.15	0.5
IPLCP	5.70×10^{-2}		
Poly5	4.96×10^{-2}		
LCP45	4.92×10^{-2}		
Poly4	4.86×10^{-2}		
IMBH	4.65×10^{-2}		
IDSP	8.24×10^{-2}	0.3	0.5
IPLCP	1.06×10^{-1}		
Poly5	8.34×10^{-2}		
LCP45	8.22×10^{-2}		
Poly4	8.03×10^{-2}		
IMBH	7.40×10^{-2}		

It is worth pointing out that $\beta = 1.76$, which is common for $\alpha = \{0.22, 0.35, 0.5\}$, plays an important role in IDSP. When α value increases the γ value requires to be reduced in-order to show effective results whereas other two design parameters of the IDSP requires same value

i.e. $\beta = 1.76$ and $n = 1$ for $\alpha = \{0.22, 0.35, 0.5\}$. Further details, regarding performance for the pulses in terms of the metrics for, $\alpha = \{0.35, 0.5\}$, are given in [Table 2](#) and [Table 3](#).

4.1 Complexity Evaluation

In OFDM-based systems, an inverse discrete Fourier transform (IDFT) is used to transform the amplitudes of the subcarriers into complex-time-domain signals, therefore, a simple design expression of a pulse shaping function is highly desirable. Here, a convolution process occurs between the modulated symbols and a pulse shaping function. Furthermore, it is studied that a simple design expression of a pulse shaping function can minimize the complexity when a convolution process takes place in a system [26]. Finally, the IDSP minimizes the complexity due to its simple design expression, given in (12). We followed similar methodology for time complexity evaluation, as done in [22, 23].

The simulation parameters given in [Table 1](#) are employed along with tic and toc command in MATLAB [27] to examine the time complexity by estimating the average elapsed time of the convolution process. Such convolution operation is based on various pulse shaping functions including IMBH [20], Poly4, Poly5 and LCP45 [21], IPLCP [22], the proposed IDSP and DSP [23], respectively. Based on stopwatch timer a function called tic command is used to record the internal time of the computer system and another function called toc command is executed to record elapsed time of the convolution operation in seconds. In other words, a particular set of instructions based on convolution operation are executed between tic and toc commands to estimate the average elapsed time.

Table 4. Specifications of a computer system used tic and toc commands

Title	Technology
Processor	Intel(R) Core(TM) i5-4570 CPU
Speed	3.20GHz
System Type	X-64-based PC
RAM	4GB
Windows	Microsoft Windows 8 Pro

Table 5. Average elapsed time of convolution process used for various Nyquist-I pulses, respectively

Pulse	Convolution
IMBH	40.23x10 ⁻⁶
IPLCP	39.26x10 ⁻⁶
Poly4	40.03x10 ⁻⁶
Poly5	40.69x10 ⁻⁶
LCP45	39.57x10 ⁻⁶
IDSP	39.30x10 ⁻⁶
DSP	39.11x10 ⁻⁶

Variations in the average elapsed time may occur due to the specifications of the computer system after executing the MATLAB commands. [Table 4](#) shows a computer system's specifications required to execute tic and toc commands. [Table 5](#) displays the average elapsed time of the convolution operation took place for various pulse shaping functions. The DSP [23] showed the lowest average elapsed time among all compared pulses. Whereas the IPLCP [22] has the second lowest average elapsed time followed by the proposed IDSP which shows the third lowest average elapsed convolution time. Here, we can say that the IDSP is desirable for OFDM-based systems because it shows a suitable reduction in the complexity of the

convolution operation due to having simple design expression in comparison to other existing pulses. However, the Poly5 [21] and IMBH [20] show highest average elapsed times which show that both the pulses have complex pulse shaping function design expressions.

5. Conclusion

A newfangled Nyquist-I pulse called improved dual sinc pulse (IDSP) is proposed to achieve the objective conditions of the pulse. The IDSP is an improved version of the DSP because the DSP was initially defined for $\alpha = 1$, whereas IDSP is defined for $0 \leq \alpha \leq 1$. In general, there are four design parameters that characterize the IDSP, including α , β , γ , and n . The parameter β manages the shape of the main lobe, whereas γ determines the phase of the pulse and magnitude of the side lobes, and n is the power of the IDSP.

We considered three important values of α i.e. $\alpha = \{0.22, 0.35, 0.5\}$, to compare and evaluate the achievements of different state-of-the-art pulse shaping functions. We determined the sub-optimum design parameters of the IDSP for $\alpha = \{0.22, 0.35, 0.5\}$ via extensive numerical and theoretical simulations. We determined the sub-optimum combinations as $\beta = 1.76$, $\gamma = 3$, and $n = 1$ for $\alpha = \{0.22\}$; $\beta = 1.76$, $\gamma = 2$ and $n = 1$ for $\alpha = \{0.35\}$; and $\beta = 1.76$, $\gamma = 1.6$, $n = 1$ for $\alpha = \{0.5\}$ in terms of the evaluated metrics. In general terms, the IDSP outperformed other existing novel pulses, including IMBH, IPLCP, Poly4, Poly5 and LCP45 in terms of the evaluated metrics for $\alpha = \{0.22, 0.35, 0.5\}$.

References

- [1] M. Elkourdi, B. Peköz, E. Güvenkaya, and H. Arslan, "Waveform Design Principles for 5G and Beyond," in *Proc. of IEEE Wireless and Microwave Technology Conference (WAMICON)*, pp. 1-6, Apr. 2016. [Article \(CrossRef Link\)](#)
- [2] A. Demir and H. Arslan, "The impact of adaptive guards for 5G and beyond," in *Proc. of IEEE International Symposium on Personal, Indoor, and Mobile Radio Communications (PIMRC)*, pp. 1-5, Oct. 2017. [Article \(CrossRef Link\)](#)
- [3] B. Farhang-Boroujeny and H. Moradi, "OFDM Inspired Waveforms for 5G," *IEEE Communications Surveys & Tutorials*, vol. 18, no. 4, pp. 2474-2492, May 2016. [Article \(CrossRef Link\)](#)
- [4] X. Yang, X. Wang, and J. Zhang, "A new waveform based on Slepian basis for 5G system," in *Proc. of IEEE International Conference on Wireless Days (WD)*, pp. 1-4, Mar. 2016. [Article \(CrossRef Link\)](#)
- [5] Z. Xie, Q. Zhu, and S. Zhao, "Resource allocation algorithm based on simultaneous wireless information and power transfer for OFDM relay networks," *KSII Transactions on Internet and Information Systems*, vol. 11, no. 12, pp. 5943-5962, Dec. 2017. [Article \(CrossRef Link\)](#)
- [6] S. Chen and J. Zhao, "The requirements, challenges, and technologies for 5G of terrestrial mobile telecommunication," *IEEE Communication Magazine*, vol. 52, no. 5, pp. 36-43, May 2014. [Article \(CrossRef Link\)](#)
- [7] T. Hwang, C. Yang, G. Wu, S. Li, and G.-Y. Li, "OFDM and its wireless applications: a survey," *IEEE Transactions on Vehicular Technology*, vol. 58, no. 4, pp. 1673-1694, May 2009. [Article \(CrossRef Link\)](#)
- [8] A.R. Reyhani, A. Farhang, and B. Farhang-Boroujeny, "Circularly pulse-shaped waveforms for 5G: Options and Comparisons," in *Proc. of IEEE Global Communications Conference (GLOBECOMM)*, pp. 1-7, Dec. 2015. [Article \(CrossRef Link\)](#)
- [9] G. Zhai and B. Shi, "Substrate integrated waveguide bandpass filter with enhancement of out-band suppression using C-shaped symmetrical slots," in *Proc. of IEEE International Conference on Signal and Image Processing (ICSIP)*, pp. 427-431, Aug. 2017. [Article \(CrossRef Link\)](#)

- [10] E. H. M. Alian and P. Mitran, "Jitter-Robust spectral shaping in OFDM," *IEEE Transactions on Communications*, vol. 63, no. 4, pp. 1282-1290, Mar. 2015. [Article \(CrossRef Link\)](#)
- [11] A. E. Loulou and M. Renfors, "Enhanced OFDM for fragmented spectrum use in 5G systems," *Transactions on Emerging Telecommunications Technologies*, vol. 26, no. 1, pp. 31-45, Jan. 2015. [Article \(CrossRef Link\)](#)
- [12] X. Wang and B. Hu, "A low-complexity ML estimator for carrier and sampling frequency offsets in OFDM systems," *IEEE Communications Letters*, vol. 18, no. 3, pp. 503-506, Mar. 2014. [Article \(CrossRef Link\)](#)
- [13] J. Lu, X. Chen, S. Liu, and P. Fan, "Location-aware ICI reduction in MIMO-OFDM downlinks for high speed railway communication systems," *IEEE Transactions on Vehicular Technology*, vol. 67, no. 4, pp. 2958-2972, Apr. 2018. [Article \(CrossRef Link\)](#)
- [14] R. Song and S. H. Leung, "A novel OFDM receiver with second order polynomial Nyquist window function," *IEEE Communications Letters*, vol. 9, no. 5, pp. 391-393, May 2005. [Article \(CrossRef Link\)](#)
- [15] Y. Li, M. Wen, X. Cheng, and L. Q. Yang, "Index modulated OFDM with ICI Self-Cancellation," in *Proc. of IEEE International Conference on Vehicular Technology Conference (VTC)*, pp. 1-5, May 2016. [Article \(CrossRef Link\)](#)
- [16] C. Y. Hsu and H. C. Liao, "Generalized precoding method for PAPR reduction with low complexity in OFDM systems," *IET Communications*, vol. 12, no. 7, pp. 796-808, May 2018. [Article \(CrossRef Link\)](#)
- [17] S. H. Wang, K. C. Lee, and C. P. Li, "A Low-Complexity architecture for PAPR reduction in OFDM systems with near-optimal performance," *IEEE Transactions on Vehicular Technology*, vol. 65, no. 1, pp. 169-179, Jan. 2016. [Article \(CrossRef Link\)](#)
- [18] D. Zabala-Blanco, G. Campuzano, and C. A. Azurdia-Meza, "BER reduction in OFDM systems susceptible to ICI using the exponential linear pulse," in *Proc. of IEEE International Conference on Electronics, Electrical Engineering and Computing (INTERCON)*, pp. 1-4, Aug. 2017. [Article \(CrossRef Link\)](#)
- [19] N. D. Alexandru and A. L. Onofrei, "ICI reduction in OFDM systems using phase modified sinc pulse," *Wireless Personal Communications*, vol. 53, no. 1, pp. 141-151, Mar. 2010. [Article \(CrossRef Link\)](#)
- [20] R. Saxena and H. D. Joshi, "ICI reduction in OFDM systems using IMBH pulse shapes," *Wireless Personal Communications*, vol. 71, no. 4, pp. 2895-2911, Aug. 2013. [Article \(CrossRef Link\)](#)
- [21] S. Kamal, C. A. Azurdia-Meza, and K. S. Lee, "Subsiding OOB Emission and ICI Power using iPOWER pulse in OFDM systems," *Advances in Electrical and Computer Engineering*, vol. 16, no. 1, pp. 79-86, Feb. 2016. [Article \(CrossRef Link\)](#)
- [22] S. Kamal, C. A. Azurdia-Meza, and K. S. Lee, "Improved Nyquist-I pulses to enhance the performance of OFDM-based systems," *Wireless Personal Communications*, vol. 95, no. 4, pp. 4095-4111, Aug. 2017. [Article \(CrossRef Link\)](#)
- [23] S. Kamal, C. A. Azurdia-Meza, and K. Lee, "Suppressing the effect of ICI power using dual sinc pulses in OFDM-based systems," *AEU-International Journal of Electronics and Communications*, vol. 70, no. 7, pp. 953-960, July 2016. [Article \(CrossRef Link\)](#)
- [24] K. N. Le, "Insight on ICI and its effects on performance of OFDM systems," *Digital Signal Processing*, vol. 18, no. 6, pp. 876-884, Nov. 2008. [Article \(CrossRef Link\)](#)
- [25] K. N. Le, "Pulse shaping of OFDM systems in AWGN channel," *Hong Kong Institute of Engineers Transactions*, vol. 15, no. 4, pp. 29-34, May 2014. [Article \(CrossRef Link\)](#)
- [26] C. Marven and G. Ewers, *A simple approach to digital signal processing*, 1st Edition, Wiley-Interscience, 1996.
- [27] C. Solomon and T. Breckon, *Fundamentals of digital image processing: A practical approach with examples in Matlab*, 1st Edition, Wiley-Blackwell, 2011.



Shaharyar Kamal received his M.S. degree in Computer Engineering from Mid Sweden University, Sweden. He obtained Ph.D. degree from the Department of Radio and Electronics Engineering at Kyung Hee University, Republic of Korea. He joined the Department of Computer Science, Air University as an Assistant professor in 2017. His research interest includes 5G and beyond, advanced wireless communication systems, internet of things and multimedia.



Hojin Kang Kim received the B.Sc. degree in Electrical Engineering from Universidad de Chile, Chile in 2019. He is currently doing his M.Sc. degree in Electrical Engineering in Universidad de Chile. His research interests include topics such as vehicular communications, machine learning applications in communications and deep learning.



Cesar A. Azurdia-Meza received the B.Sc. degree in Electronics Engineering from Universidad del Valle de Guatemala, Guatemala in 2005, and the M.Sc. degree in Electrical Engineering from Linnaeus University, Sweden in 2009. In 2013 he obtained the Ph.D degree in Electronics and Radio Engineering, Kyung Hee University, Republic of Korea. He joined the Department of Electrical Engineering, University of Chile as an Assistant Professor in August 2013, where he is currently lecturing on wireless and mobile communication systems. He has served as Technical Program Committee (TPC) member for multiple conferences, as well as a reviewer in journals such as IEEE Communications Letters, IEEE Transactions on Wireless Communications, Wireless Personal Communications, IEEE Access, IET Communications, EURASIP Journal on Advances in Signal Processing, among others. Dr. Azurdia is an IEEE Communications Society Member, as well as Member of the IEICE Communications Society. His research interests include topics such as Nyquist's ISI criterion, OFDM-based systems, SC-FDMA, visible light communication systems, vehicular communications, 5G and beyond enabling technologies, and signal processing techniques for communication systems. He is a co-recipient of the 2019 IEEE LATINCOM Best Paper Award, as well as the 2016 IEEE CONESCAPAN Best Paper Award.



Dong-Seong Kim received his Ph.D. degree in Electrical and Computer Engineering from the Seoul National University, Seoul, Korea, in 2003. From 1994 to 2003, he worked as a full-time researcher in ERC-ACI at Seoul National University, Seoul, Korea. From March 2003 to February 2005, he worked as a postdoctoral researcher at the Wireless Network Laboratory in the School of Electrical and Computer Engineering at Cornell University, NY. From 2007 to 2009, he was a visiting professor with Department of Computer Science, University of California, Davis, CA. He is currently a dean and director of industrial academic cooperation foundation and ICT Convergence Research Center(Grand ICT center and NRF advanced research center program) supported by Korean government at Kumoh National Institute of Technology. He is a senior member of IEEE and ACM. His current main research interests are real-time IoT and smart platform, industrial wireless control network, networked embedded system and Fieldbus.